Inorganic Chemistry

ARTICLE

pubs.acs.org/IC

New Phenoxido-Bridged Quasi-Tetrahedral and Rhomboidal [Cu_4] Compounds Bearing μ_4-Oxido or $\mu_{1,1}$-Azido Ligands: Synthesis, Chemical Reactivity, and Magnetic Studies

Mrinal Sarkar,[†] Rodolphe Clérac,[*,‡,§] Corine Mathonière,[⊥] Nigel G. R. Hearns,[‡,§] Valerio Bertolasi,[∥] and Debashis Ray[*,†]

[†]Department of Chemistry, Indian Institute of Technology, Kharagpur 721 302, India

[‡]CNRS, UPR 8641, Centre de Recherche Paul Pascal (CRPP), Equipe "Matériaux Moléculaires Magnétiques", 115 avenue du Dr. Albert Schweitzer, Pessac F-33600, France

[§]Université de Bordeaux, UPR 8641, Pessac F-33600, France

[⊥]CNRS, Université de Bordeaux, ICMCB, 87 avenue du Dr. A. Schweitzer, Pessac F-33608, France

[∥]Dipartimento di Chimica e Centro di Strutturistica Diffrattometica, Università di Ferrara, Via Borsari 46, 44100 Ferrara, Italy

Supporting Information

ABSTRACT: [$Cu_2(\mu_4\text{-}O)Cu_2$] and [$Cu_2(\mu_{1,1}\text{-}N_3)_4Cu_2$] geometrical arrangements are found in a new family of tetranuclear copper(II) complexes: [$Cu_4(\mu_4\text{-}O)(\mu\text{-cip})_2Cl_4$] (**1**), [$Cu_4(\mu_4\text{-}O)(\mu\text{-cip})_2(\mu_{1,3}\text{-}O_2CPh)_4]\cdot 2CH_3OH$ (**2**·$2CH_3OH$), and [$Cu_4(\mu_{1,1}\text{-}N_3)_4(\mu\text{-cip})_2(N_3)_2]\cdot$DMF (**3**·DMF) [Hcip = 2,6-bis(cyclohexyliminomethylene)-4-methylphenol; CH_3OH = methanol; DMF = dimethylformamide]. These complexes have been characterized by X-ray crystallography, and their magnetic properties have been studied. **1** and **2** form quasi-tetrahedral [$Cu_4(\mu_4\text{-}O)$] complexes, and **3** is the first example of a rhomboidal [$Cu_4(\mu_{1,1}\text{-}N_3)$] compound. Formation of the [Cu_4] compounds is achieved via ligand-exchange reactions. The relative binding strength of the three ancillary ligands as N_3^- > $PhCO_2^-$ > Cl^- has been demonstrated from the core-conversion and peripheral ligand-exchange reactions. For the three complexes, the magnetic susceptibility measurements in the range of 1.8−300 K have been performed and modeled using two isolated $S = {}^1/_2$ dimers based on the spin Hamiltonian $H = -2J\{S_{Cu,1}\cdot S_{Cu,2}\}$ with $J/k_B = -513$, -340, and -315 K for **1**−**3**, respectively (where J is the exchange constant through the oxido−phenoxido and azido−phenoxido bridges, respectively).

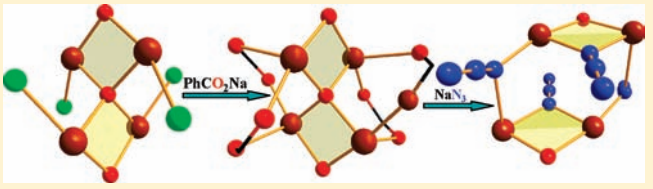

INTRODUCTION

During the last 2 decades, the synthesis and characterization of polynuclear transition-metal aggregates have received considerable interest because of their importance for examples as magnetic materials, bioinorganic model compounds, and catalysts.[1−3] The self-assembly of small building units with coligands can be used to synthesize polynuclear compounds with controlled aggregation. The strong and highly directional metal−ligand interactions can effectively be used in lieu of several weak interactions (like hydrogen-bonding and $\pi-\pi$ interactions) to direct the formation of polynuclear coordination compounds. The role of the ligand geometry and the tuning of the reaction conditions with transition-metal ions are crucial to identify and direct the aggregation process. Phenoxido-bridged [Cu_2] fragments have quite often been studied as chemical models for magnetic exchange interactions[4−6] and as building units for the construction of tetra- and polynuclear complexes exhibiting interesting magnetic properties.[7−12] Recently, our research work has been devoted to the preparation of a new family of [Cu_4] aggregates based on the phenoxido-bridged [Cu_2] units. The tendency of the Cu^{II} ions to accept a fifth coordinating group in the *apical* position and the ability of the phenoxido ligands to bridge metal ions make the association of dinuclear [Cu_2] moieties into discrete oligo- and polynuclear complexes possible.

The assembly of two dinuclear [Cu_2] units depends on the number and nature of secondary bridging or coordinating groups present in various reactions in such a way that four types of [Cu_4] aggregates can be obtained with cubane, tetrahedron, stepped-cubane, rhomboid, and double-cubane geometry. Out of these various aggregation possibilities, cubane, stepped-cubane, and double-cubane assemblies were not formed in the present work (Scheme 1). Among the ancillary ligands used, azido and carboxylato groups have been employed because of their versatile bridging modes (Scheme 2). The carboxylato group can adopt numerous bridging conformations like the syn−syn, syn−anti, anti−anti, and μ_3-1,1,3-modes, and depending upon the two binding positions (*basal* or *apical*) around Cu^{II} ions, these bridging modes can mediate a large variety of exchange interactions. Quite generally, syn−syn and syn−anti configurations favor

Received: November 12, 2010
Published: April 04, 2011

   dx.doi.org/10.1021/ic102226j | *Inorg. Chem.* 2011, 50, 3922–3933

Scheme 1. Different Tetranuclear Copper Assemblies Depending on the Precursors and Ancillary Ligands

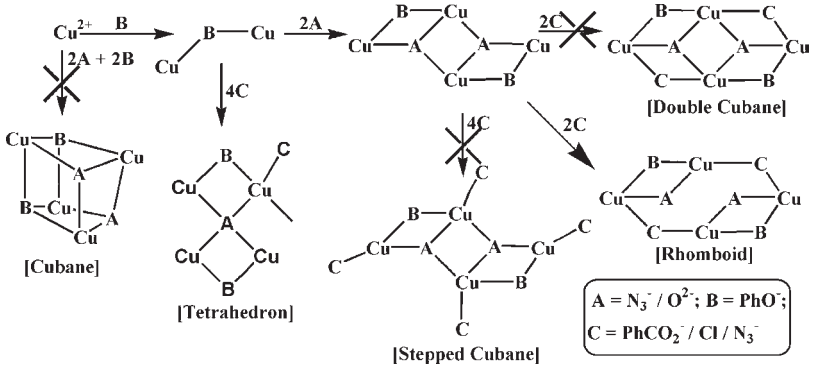

Scheme 2. Different Bridging Modes of Azido and Carboxylato Anions

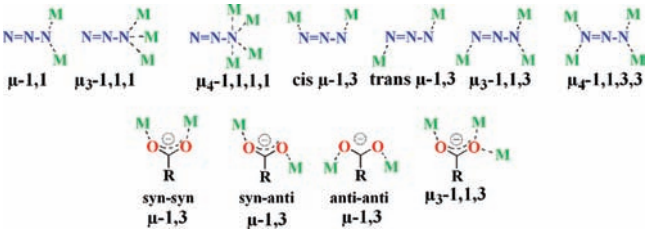

assemblies with antiferromagnetic interactions, while anti−anti mode induces medium-to-weak antiferromagnetic or ferromagnetic interactions.[13−15] As a result of extensive research over the last 2 decades, the superexchange mechanisms through various bridging modes of azide are now well established. For example, symmetric μ-1,3-copper(II) azide complexes are strongly antiferromagnetic, whereas copper(II) complexes with double-symmetric μ-1,1 azide bridges are strongly ferromagnetic, provided that the Cu−N_{azide}−Cu angle is less than 108°. Usually asymmetric μ-1,3 azido bridges lead to weak antiferromagnetic coupling, whereas asymmetric μ-1,1 azide bridges propagate weak-to-moderately strong ferromagnetic or antiferromagnetic interactions.[16] In trying to prepare and study new types of $[Cu_4]$ aggregates, we have been interested in exploring the reactivity of the tetradentate phenoxide Schiff-base ligand 2,6-(cyclohexyliminomethylene)-4-methylphenol, abbreviated Hcip (Scheme 3),[17] with $Cu(NO_3)_2\cdot 3H_2O$ in the presence of additional ligands like Cl^-, $PhCO_2^-$, and N_3^-. It is worth noting that the use of one closely related ligand of Hcip, named H_3bemp (Scheme 3, right, 2,6-bis[(2-hydroxyethylimino)methyl]-4-methylphenol), led to interesting systems, consisting of $[Co_4]$,[18] $[Ni_6]$,[19] and $[Cu_{18}]$[20] complexes and a heterobimetallic $[Mn_6Cu_{10}]$[21] aggregate. Herein, three new $[Cu_4]$ complexes based on the cip^- anionic ligand are reported: **1** and **2**·2CH_3OH, both containing a central tetrahedral μ_4-oxido anion to stabilize tetrahedral complexes and a bridged bis-N_3 rhomboid compound, **3**·DMF. These complexes have been isolated and crystallographically characterized, and their magnetic properties have been studied.

EXPERIMENTAL SECTION

Materials. The chemicals used were obtained from the following sources: copper nitrate trihydrate, potassium chloride, sodium azide, and cyclohexylamine from SRL (India) and sodium benzoate from SD Fine Chemicals (India). All other chemicals and solvents were reagent-grade materials and were used as received without further purification. ***Caution!*** *Azide complexes of metal ions involving organic ligands are potentially explosive. Only small quantities of the complexes should be prepared, and these should be handled with care.*

Scheme 3. Hcip and Related H_3bemp Ligands

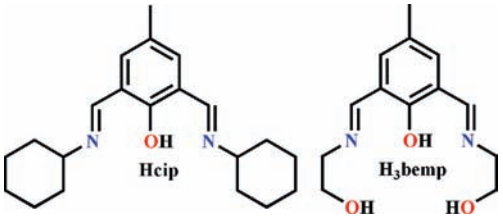

Syntheses. *Hcip Ligand.* The Hcip Schiff-base ligand was prepared from the single-step condensation of 2,6-diformyl-4-methylphenol (1.640 g, 10 mmol) and cyclohexylamine (2.29 mL, 20 mmol) in methanol (40 mL) under reflux for 1 h as reported previously.[17]

*$[Cu_4(\mu_4\text{-}O)(\mu\text{-}cip)_2Cl_4]$ (**1**).* $Cu(NO_3)_2\cdot 3H_2O$ (0.483 g, 2.00 mmol) dissolved in methanol (25 mL) was added dropwise with stirring to a yellow CH_3OH solution (15 mL) of Hcip (0.326 g, 1.00 mmol). The brown solution, formed initially, changes to green in about 5 min. After about 10 min of stirring, solid KCl (0.298 g, 4.0 mmol) was added to the reaction. The green solution was further stirred for 1 h, and a green precipitate appeared. The obtained green precipitate was collected by filtration, washed with cold methanol followed by water, and dried under vacuum over P_4O_{10}. Green single crystals suitable for X-ray analysis were obtained from a CH_2Cl_2−CH_3OH solvent mixture after 5 days. Yield: 0.398 g, 75%. Anal. Calcd for $C_{42}H_{58}N_4O_3Cl_4Cu_4$ (1062.94 g mol^{-1}): C, 47.45; H, 5.49; N, 5.27. Found: C, 47.12; H, 5.32; N, 5.01. Selected FTIR bands (KBr, cm^{-1}; s = strong, m = medium, and br = broad): 3447 (br), 1633 (s), 1559 (s), 1458 (m), 1348 (m), 1038 (m), 622 (m), 564 (m), 502 (m). Molar conductance, Λ_M (CH_2Cl_2 solution): 3.0 Ω^{-1} cm^2 mol^{-1}. UV−vis spectra [λ_{max}, nm (ε, L mol^{-1} cm^{-1})] (CH_2Cl_2 solution): 728 (688), 373 (5879), 256 (21 632).

*$[Cu_4(\mu_4\text{-}O)(\mu\text{-}cip)_2(\mu_{1,3}\text{-}O_2CPh)_4]\cdot 2CH_3OH$ (**2**·2CH_3OH)*

Method A via a Direct Route. Compound **2** was prepared by the same method as that used for **1**, only replacing KCl with $PhCO_2Na$. Green single crystals suitable for X-ray analysis were obtained from a CH_2Cl_2−CH_3OH solvent mixture after 7 days. Yield: 0.534 g, 76%. Anal. Calcd for $C_{72}H_{86}N_4O_{13}Cu_4$ (1469.67 g mol^{-1}): C, 58.84; H, 5.89; N, 3.81. Found: C, 58.61; H, 5.78; N, 3.67. Selected FTIR bands (KBr, cm^{-1}; vs = very strong, s = strong, m = medium, and br = broad):

dx.doi.org/10.1021/ic102226j |Inorg. Chem. 2011, 50, 3922–3933

3430 (br), 1624 (s), 1606 (s), 1569 (s), 1460 (m), 1372 (vs), 1063 (m), 717 (s), 678 (m), 625 (m), 503 (m). Molar conductance, Λ_M (CH_2Cl_2 solution): 3.0 Ω^{-1} cm^2 mol^{-1}. UV−vis spectra [λ_{max}, nm (ε, L mol^{-1}cm^{-1})] (CH_2Cl_2 solution): 681 (241), 378 (5033), 353 (3682), 248 (21 613).

Method B via Anion Exchange of ***1***. The green suspension of **1** (0.265 g, 0.25 mmol) in CH_3OH (25 mL) was stirred for about 5 min before the addition of $PhCO_2Na$ (0.144 g, 1.0 mmol) at ambient temperature. During the reaction, noticeable changes were observed from a green suspension to a green solution followed by the appearance of a green precipitate, which was collected by filtration, washed with cold methanol, and dried under vacuum over P_4O_{10}. Yield: 0.224 g, 64%. Anal. Calcd for $C_{72}H_{86}N_4O_{13}Cu_4$ (1469.67 g mol^{-1}): C, 58.84; H, 5.89; N, 3.81. Found: C, 58.46; H, 5.73; N, 3.64. Selected FTIR bands (KBr, cm^{-1}; s = strong, m = medium, and br = broad): 3447 (br), 1624 (s), 1605 (s), 1570 (s), 1460 (m), 1371 (vs), 1063 (m), 717 (s), 678 (m), 625 (m), 504 (m). Molar conductance, Λ_M (CH_2Cl_2 solution): 3.0 Ω^{-1} cm^2 mol^{-1}. UV−vis spectra [λ_{max}, nm (ε, L mol^{-1} cm^{-1})] (CH_2Cl_2 solution): 681 (211), 378 (4406), 353 (3223), 248 (18 922).

*[Cu$_4$($\mu_{1,1}$-N$_3$)$_4$(μ-cip)$_2$(N$_3$)$_2$]·DMF (****3****·DMF)*

Method A via a Direct Route. Compound **3** was prepared by the same method as that used for **1**, only replacing KCl with NaN_3. The obtained brown precipitate was collected by filtration, washed with cold methanol followed by water, and dried under vacuum over P_4O_{10}. Brown single crystals suitable for X-ray analysis were obtained from DMF after 5 days. Yield: 0.416 g, 72%. Anal. Calcd for $C_{45}H_{65}N_{23}O_3Cu_4$ (1230.35 g mol^{-1}): C, 43.93; H, 5.32; N, 26.18. Found: C, 43.89; H, 5.01; N, 25.86. Selected FTIR bands (KBr, cm^{-1}, vs = very strong, s = strong, m = medium, and w = weak): 2929 (vs), 2854 (vs), 2084 (vs), 2045 (vs), 1638 (vs), 1563 (vs), 1342 (s), 1041 (m), 829 (m), 765 (w). Molar conductance, Λ_M (DMF solution): 6 Ω^{-1} cm^2 mol^{-1}. UV−vis spectra [λ_{max}, nm (ε, L mol^{-1} cm^{-1})] (DMF solution): 695 (567), 380 (15 950), 301 (9540), 273 (19 240).

Method B from ***1***. The green solution of **1** (0.265 g, 0.25 mmol) in CH_2Cl_2 (25 mL) was stirred for about 5 min followed by a dropwise addition of NaN_3 (0.097 g, 1.50 mmol) dissolved in CH_3OH (20 mL) at ambient temperature. During the reaction, the solution changed color from green to brown before the appearance of a brown precipitate, which was collected by filtration, washed with cold methanol, and dried under vacuum over P_4O_{10}. Yield: 0.196 g, 68%. Anal. Calcd for $C_{45}H_{65}N_{23}O_3Cu_4$ (1230.35 g mol^{-1}): C, 43.93; H, 5.32; N, 26.18. Found: C, 43.12; H, 4.97; N, 25.64. Selected FTIR bands (KBr, cm^{-1}, vs = very strong, s = strong, m = medium, and w = weak): 2929 (vs), 2854 (vs), 2082 (vs), 2055 (vs), 1639 (vs), 1564 (vs), 1342 (s), 1042 (m), 829 (m), 766 (w). Molar conductance, Λ_M (DMF solution): 6 Ω^{-1} cm^2 mol^{-1}. UV−vis spectra [λ_{max}, nm (ε, L mol^{-1}cm^{-1})] (DMF solution): 695 (583), 380 (16 400), 301 (9809), 273 (19 783).

Method C from ***2***. Compound **3** can also be prepared from **2** using method B but replacing complex **1** by **2**. Yield: 0.190 g, 66%. Anal. Calcd for $C_{45}H_{65}N_{23}O_3Cu_4$ (1230.35 g mol^{-1}): C, 43.93; H, 5.32; N, 26.18. Found: C, 43.02; H, 5.11; N, 25.76. Selected FTIR bands (KBr, cm^{-1}, vs = very strong, s = strong, m = medium, w = weak): 2928 (vs), 2854 (vs), 2082 (vs), 2055 (vs), 1639 (vs), 1563 (vs), 1342 (s), 1042 (m), 829 (m), 765 (w). Molar conductance, Λ_M (DMF solution): 6 Ω^{-1} cm^2 mol^{-1}. UV−vis spectra [λ_{max}, nm (ε, L mol^{-1} cm^{-1})] (DMF solution): 695 (533), 380 (14 993), 301 (8968), 273 (18 086).

Physical Measurements. Elemental analyses (C, H, and N) were performed with a Perkin-Elmer model 240C elemental analyzer. Fourier transform infrared (FTIR) spectra were recorded on a Perkin-Elmer 883 spectrometer. The solution electrical conductivity and electronic spectra were obtained using a Unitech type U131C digital conductivity meter with a solute concentration of about 10^{-3} M and a Shimadzu UV 3100 UV−vis−near-IR spectrophotometer, respectively. The powder X-ray diffraction (PXRD) patterns were obtained using a Philips PW 1710 diffractometer with Cu Kα radiation. The magnetic susceptibility measurements were obtained with the use of a Quantum Design MPMS-XL magnetometer housed at the Centre de Recherche Paul Pascal. This magnetometer works between 1.8 and 300 K for direct-current (dc) applied fields ranging from −7 to 7 T. Measurements were performed on polycrystalline samples of 14.34, 10.26, and 30.82 mg for **1**, **2**·2CH_3OH, and **3**·DMF, respectively. The magnetic data were corrected for the sample holder and the diamagnetic contributions.

Crystal Data Collection and Refinement for ***1***, ***2***·*2CH$_3$OH, and* ***3***·*DMF.* Single-crystal data of complexes **1**, **2**·2CH_3OH, and **3**·DMF were collected on a Bruker APEX-2 CCD X-ray diffractometer using graphite-monochromated Mo Kα radiation (λ = 0.7107 Å). Data were collected at 293 K. The refinement was performed anisotropically using full-matrix least squares with all non-H atoms. The H atoms were included on calculated positions, riding on their carrier atoms. The hydroxy H atom O2−H was found in the difference Fourier maps and refined with a O−H fixed distance of 0.90 Å. The crystal parameters and other experimental details of data collection are summarized in Table 1.

RESULTS AND DISCUSSION

Synthetic Considerations. The Schiff-base ligand 2,6-bis-(cyclohexyliminomethylene)-4-methylphenol (Hcip) was prepared (Scheme S1 in the Supporting Information) following a literature procedure,[17] and its reactions with copper(II) salts have been systematically investigated, as summarized in Scheme 4. When the reaction of $Cu(NO_3)_2\cdot 3H_2O$ was carried out with Hcip in CH_3OH in the presence of KCl and in the absence of base, **1** was obtained (Scheme 4). Several Cu/Hcip ratios were explored, and we report here only the optimized ones that gave clean and characterizable products in high yield. At room temperature, complex **1** is easily isolated by stirring a methanolic solution of $Cu(NO_3)_2\cdot 3H_2O$, KCl, and Hcip in a 2:2:1 molar ratio for 1 h. The complex precipitates directly from the reaction mixture as a green solid in ∼75% yield. The preparation of **1** is summarized by eq 1, accounting for the formation of the oxido bridge from a water molecule. It is worth mentioning that the use of $CuCl_2\cdot 2H_2O$ instead of $Cu(NO_3)_2\cdot 3H_2O$ leads also directly to the synthesis of **1**.

$$2\text{Hcip} + 4\text{Cu}(\text{NO}_3)_2\cdot 3\text{H}_2\text{O} + 4\text{KC1} \rightarrow [\text{Cu}_4(\mu_4\text{-O})(\mu\text{-cip})_2\text{Cl}_4] + 4\text{KNO}_3 + 4\text{HNO}_3 + 11\text{H}_2\text{O} \quad (1)$$

The elemental analysis and molar conductivity data are consistent with the formula $[Cu_4(\mu_4\text{-O})(\mu\text{-cip})_2Cl_4]$ for **1**. However, no sign of the formation of phenoxido-bridged $[Cu_2]$ dinuclear species was observed because of the better stability of **1**, which crystallizes with a central μ_4-oxido group to assemble a pair of $[Cu_2]$ units (vide infra). This synthetic procedure was further explored with NaO_2CPh and NaN_3 successively in place of KCl. Green crystals of **2** and brown crystals of **3** (Scheme 4) were directly synthesized in ∼70% yield in CH_3OH by stirring reaction solutions of $Cu(NO_3)_2\cdot 3H_2O$, Hcip, and $PhCO_2Na$ or NaN_3 in a 2:1:2 or 2:1:3 molar ratio for 1 h under aerobic conditions at room temperature. For **2**, the same reactions in the presence of a stoichiometric addition of either NEt_3 or NaOH gave the same product, confirming the formation of hydroxido bridges independently of the type and nature of the base. The direct syntheses of **2** and **3** from Hcip are summarized in eqs 2 and 3. It is interesting to note that **2** can also be obtained from the

Table 1. Crystallographic Data for 1, 2·2CH$_3$OH, and 3·DMF

compound	**1**	**2**·2CH$_3$OH	**3**·DMF
formula	$C_{42}H_{58}N_4O_3Cl_4Cu_4$	$C_{72}H_{86}N_4O_{13}Cu_4$	$C_{45}H_{65}N_{23}O_3Cu_4$
M	1062.94	1469.67	1230.35
space group	$I4_1/a$	$C2/c$	$C2/c$
cryst syst	tetragonal	monoclinic	monoclinic
a/Å	12.6302(5)	15.0640(19)	17.6314(10)
b/Å	12.6302(5)	35.820(5)	16.5650(10)
c/Å	28.8439(12)	13.1134(17)	19.2469(11)
α/deg	90.0	90.0	90.0
β/deg	90.0	103.036(4)	103.887(2)
γ/deg	90.0	90.0	90.0
V/Å^3	4601.2(3)	6893.5(15)	5457.0(5)
T/K	293	293	293
Z	4	4	4
D_c/g cm^{-3}	1.534	1.408	1.498
F(000)	2184	3032	2544
μ(Mo Kα)/cm^{-1}	20.97	12.82	16.00
measd reflns	28 248	49 833	37 353
unique reflns	4129	9743	6493
R_{int}	0.0325	0.0470	0.0503
obsd reflns [$I \geq 2\sigma(I)$]	2702	6754	4523
$\theta_{min}-\theta_{max}$/deg	1.76−32.88	1.14−29.74	1.71−28.00
h; k; l ranges	−15, +17; −16, +19; −42, +44	−20, +20; −49, +41; −18, +17	−23, +23; −21, +21; −24, +23
$R(F^2)$ (obsd reflns)	0.0488	0.0589	0.0430
w$R(F^2)$ (all reflns)	0.2282	0.1805	0.1186
no. of variables	131	424	337
GOF	0.844	1.078	1.007
$\Delta\rho_{max}$; $\Delta\rho_{min}$ (e Å^{-3})	1.028; −0.943	2.531; −0.566	0.559; −0.370

$Cu(O_2CPh)_2 \cdot H_2O$ precursor.

$$2Hcip + 4Cu(NO_3)_2 \cdot 3H_2O + 4PhCO_2Na \rightarrow [Cu_4(\mu_4\text{-}O)(\mu\text{-}cip)_2(\mu\text{-}O_2CPh)_4] + 4HNO_3 + 4NaNO_3 + 11H_2O \quad (2)$$

$$2Hcip + 4Cu(NO_3)_2 \cdot 3H_2O + 6NaN_3 \rightarrow [Cu_4(\mu\text{-}N_3)_4(\mu\text{-}cip)_2(N_3)_2] + 2HNO_3 + 6NaNO_3 + 12H_2O \quad (3)$$

The elemental analysis and molar conductivity data confirm the respective formula of the two compounds. The nature of the final complex is greatly influenced by the presence of the ligands, solvent, and sequence of the addition of the reactants. Weakly coordinating anions such as Cl^- and $PhCO_2^-$ in both nonbridging and bridging modes support the μ_4-O-bridged cores in **1** and **2**, respectively. As for **1**, the formation of dinuclear phenoxido-bridged [Cu_2] species was not observed, suggesting a better stability of the μ_4-O- and μ-N_3-bridged [Cu_4] complexes. As illustrated by the synthesis of **1**−**3**, reactions between the Hcip ligand and copper(II) salts lead to different self-assemblies depending on the nature of the additional ligands. Therefore, the formation of these three [Cu_4] complexes can be directly controlled by choosing the right ancillary ligands, N_3^-, $PhCO_2^-$, and Cl^-, and their relative binding strength can be studied from ligand-exchange reactions.

Ligand-Exchange Reactivity Studies on Complex ***1***. As summarized by eq 4, **2** can be easily obtained by reacting **1** with sodium benzoate in methanol. Treatment of a green suspension of **1** in CH_3OH by sodium benzoate shifts the equilibrium in favor of **2** with noticeable dissolution of the suspension to a clear green solution followed by precipitation of **2** within 5 min. The precipitate was filtered, washed with CH_3OH, dried, and dissolved in CH_2Cl_2 for crystallization and layered with CH_3OH. Green crystals of **2** grew slowly over several days and were isolated by filtration.

$$[Cu_4(\mu_4\text{-}O)(\mu\text{-}cip)_2Cl_4] + 4PhCO_2Na \rightarrow [Cu_4(\mu_4\text{-}O)(\mu\text{-}cip)_2(\mu\text{-}O_2CPh)_4] + 4NaCl \quad (4)$$

The mechanism of the conversion of **1** to **2** is relatively straightforward. During this reaction, terminal chlorides are exchanged by bridging bidentate benzoates in the *equatorial* and *apical* sites of the four Cu^{II} centers without affecting the central μ_4-oxido core structure. Concomitantly, the four Cu^{II} ions switch from a square-planar to a square-pyramidal geometry.

Transformation of the [Cu$_4$(μ$_4$-O)] Tetrahedral Species to a [Cu$_4$(μ-N$_3$)$_4$] Rhomboidal Complex. The strength and nature of the binding ability of the three ancillary ligands Cl^-, $PhCO_2^-$, and N_3^- together with the plasticity of the copper coordination geometries can be discussed considering the three compounds and their interconversions. The replacement of both oxido and chlorido groups or both oxido and benzoato groups in **1** and **2**, respectively, by azido ligands leads to transformation of the

dx.doi.org/10.1021/ic102226j |*Inorg. Chem.* 2011, 50, 3922–3933

Scheme 4. Schematic Representation of the Different [Cu_4] Assemblies Obtained in This Work

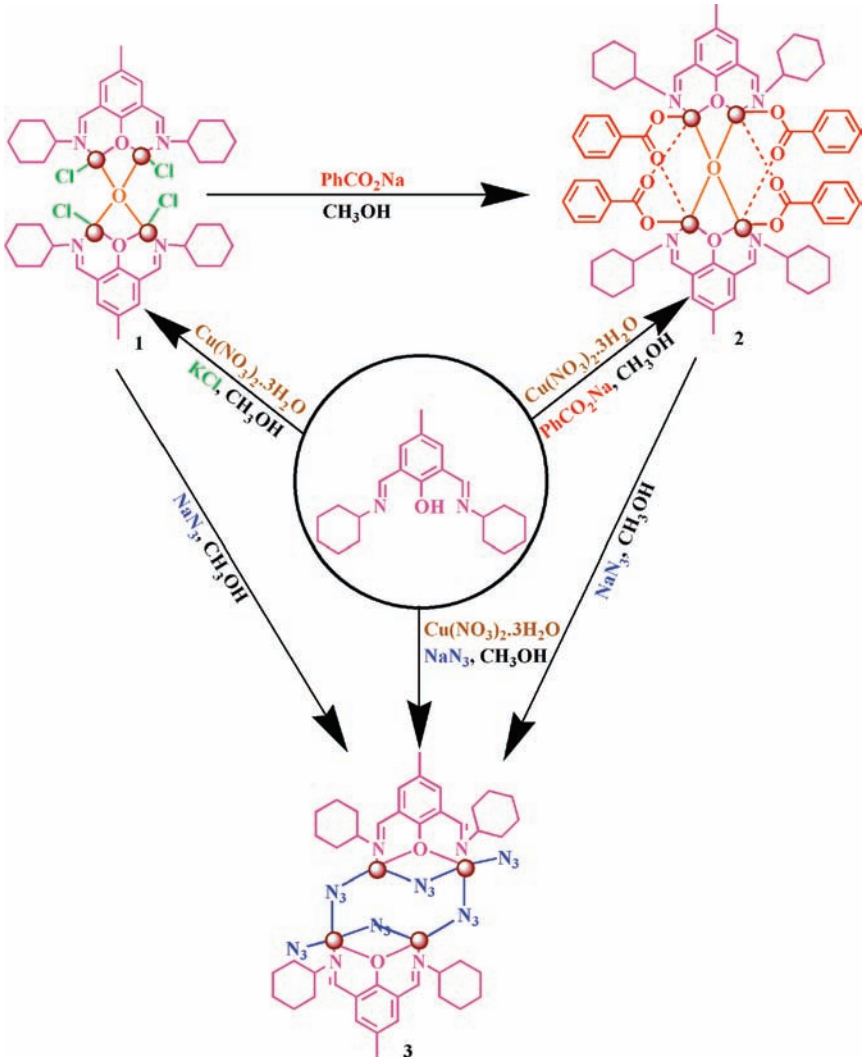

[$Cu_4(\mu_4\text{-O})$] tetrahedral cores into a new [Cu_4] assembly. At ambient temperature and in air, the treatment of **1** or **2** by 6 equiv of sodium azide in methanol or CH_2Cl_2−CH_3OH (1:1) favors the formation of **3** with a characteristic change of color from green to brown followed by precipitation of a brown solid within 10 min. The precipitate was filtered, washed with CH_3OH, dried, and dissolved in DMF for crystallization. Brown crystals of **3** formed slowly over several days and were isolated by filtration. During conversions of **1** to **3** and **2** to **3**, all of the terminal ligands are exchanged by three different types of azide anions: two types of $\mu_{1,1}$-N_3^- and terminal N_3^- ligands. The mechanism of such conversions is clearly complicated because it involves the following: (i) in **1**, abstraction of peripheral chlorido anions by azido groups together with substitution of the μ_4-oxido center by two $\mu_{1,1}$-N_3^- bridges, leading to a change of the coordination sphere for two Cu^{II} sites from square-planar to square-pyramidal geometry; (ii) in **2**, the central μ_4-oxido bridge and the benzoato groups are exchanged in a similar fashion. Abstraction of central μ_4-oxido ions by $\mu_{1,1}$-N_3^- bridges triggers the structural change from a tetrahedral [$Cu_4(\mu_4\text{-O})$] form to a rhomboidal [$Cu_4(\mu\text{-}N_3)_4$] complex. Considering the quantitative and spontaneous conversions of **1** to **2** (eq 4), **1** to **3** (eq 5), and **2** to **3** (eq 6), the relative binding strength of the three ligands can be established without ambiguity: $N_3^- > PhCO_2^- > Cl^-$.

$$[Cu_4(\mu_4\text{-O})(\mu\text{-cip})_2Cl_4] + 6NaN_3 + H_2O \rightarrow$$

$$[Cu_4(\mu\text{-}N_3)_4(\mu\text{-cip})_2(N_3)_2] + 2NaOH + 4NaCl \quad (5)$$

$$[Cu_4(\mu_4\text{-O})(\mu\text{-cip})_2(\mu\text{-}O_2CPh)_4] + 6NaN_3 + H_2O \rightarrow$$

$$[Cu_4(\mu\text{-}N_3)_4(\mu\text{-cip})_2(N_3)_2] + 2NaOH + 4PhCO_2Na \quad (6)$$

Ligand-exchange and core-conversion reactions have been identified by FTIR measurement, solubility differences, and the checking of unit cell parameters and crystal systems of grown single crystals from powder samples (the resulting IR spectra are given in the Supporting Information). PXRD data have been taken to identify the phase change from **1** to **2** or **3** and **2** to **3** conversions. The PXRD patterns of the three complexes are shown in Figure S1 in the Supporting Information. These patterns are consistent with those of the simulated ones obtained from the single-crystal X-ray diffraction data.

dx.doi.org/10.1021/ic102226j |*Inorg. Chem.* 2011, 50, 3922–3933

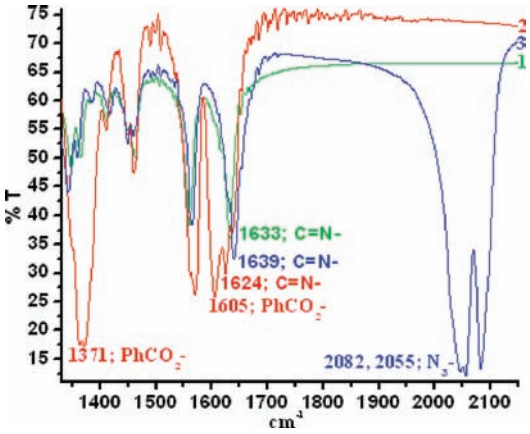

Figure 1. FTIR spectra of **1**, **2**·2CH_3OH, and **3**·DMF between 1330 and 2150 cm^{-1}.

FTIR Spectra. The three $[Cu_4]$ complexes show characteristic bands of the Cu^{II}-bound cip^- ligands. $\bar{\nu}_{C=N}$ stretching modes are observed at 1624−1639 cm^{-1} for **1**−**3**. For **2**, the asymmetric and symmetric stretching vibrations of the four bound carboxylate groups are detected at 1605 cm^{-1} as $\bar{\nu}_{as(COO)}$, while $\bar{\nu}_{s(COO)}$ appeared at 1371 cm^{-1}. The difference, $\Delta\bar{\nu}$ = 234 cm^{-1}, is in accordance with the presence of $\mu_{1,3}$-bridging carboxylates in **2**. From the above $\Delta\bar{\nu}$ value, we can conclude that the benzoate anions act as bidentate anions bridging two metal ion sites. For nonbridging carboxylato coordination, this $\Delta\bar{\nu}$ separation is usually larger (ca. 350 cm^{-1}).[22] In the spectra of **1** and **2**, two medium absorption bands at 622 and 625 cm^{-1} were detected, respectively. These bands are missing in the spectra of the free ligand, KCl, sodium benzoate, or copper(II) nitrate. These bands are associated with $\bar{\nu}_{Cu-O}$ vibrations originating from the $[Cu_4O]$ core. Recently, we have reported this $[Cu_4O]$ band at 566 cm^{-1} for $[Cu_4(\mu_4\text{-}O)(bahped)_2](ClO_4)_2$,[23] while in the case of $[Cu_4Cl_4(\mu_4\text{-}O)(OSR_2)_4]$ (R = Et, ^{n}Bu)[24] and copper 2,6-bis(morpholinomethyl)-4-methylphenol complexes,[25] the $\bar{\nu}_{Cu-O}$ vibrations are observed at 581−592 cm^{-1}. In addition, **3** exhibits a strong band at ∼2082 cm^{-1}, which splits into three components, and another strong band at 2055 cm^{-1}. These bands can be easily assigned to the asymmetric stretching mode of the two different types of azide ligands. Finally, the band at 1342 cm^{-1} corresponds to the $\bar{\nu}_{sym}$ stretching vibration of the N_3^- groups.[26]

The conversion of **1** to **2** or **3** and **2** to **3** in solution has been well monitored using FTIR spectroscopy and the characteristic bands of complexes **1**−**3** (Figure 1).

Electronic UV−Vis Spectra. The three complexes in CH_2Cl_2 solutions show multiple bands in the 200−900 nm region. Broad absorption bands (λ), with maxima at 728 nm (ε = 688 L mol^{-1} cm^{-1}), 681 nm (ε = 241 L mol^{-1} cm^{-1}), and 695 nm (ε = 567 L mol^{-1} cm^{-1}) for **1**−**3**, respectively, are induced by the cip ligand. The intense absorptions below 400 nm at 256 nm (ε = 21 632 L mol^{-1} cm^{-1}), 248 nm (ε = 21 613 L mol^{-1} cm^{-1}), and 273 nm (ε = 19 240 L mol^{-1} cm^{-1}) are dominated by metal-to-ligand charge-transfer transitions for **1**, **2**·2CH_3OH, and **3**·DMF, respectively. Spectra of these complexes also show shoulders at 373 nm (ε = 5879 L mol^{-1} cm^{-1}), 378 nm (ε = 5053 L mol^{-1} cm^{-1}), and 380 nm (ε = 15 950 L mol^{-1} cm^{-1}), respectively, due to $HO^- \rightarrow Cu^{II}$ and $PhO^- \rightarrow Cu^{II}$ ligand-to-metal charge-transfer transitions.[27]

Table 2. Selected Interatomic Distances (Å) and Angles (deg) for Complex 1[a]

		Distances	
Cl1−Cu1	2.2437(10)	Cu1−O1	1.9670(18)
O2−Cu1*1	1.9084(3)	Cu1−N1	1.968(2)
O2−Cu1*2	1.9084(3)	Cu1−Cu1*1	2.9947(7)
O2−Cu1*3	1.9084(3)	O1−Cu1*1	1.9670(18)
O2−Cu1	1.9084(3)		
		Angles	
O2−Cu1−O1	78.74(6)	O2−Cu1−Cl1	89.00(3)
O2−Cu1−N1	169.99(8)	O1−Cu1−Cl1	158.20(6)
O1−Cu1−N1	91.99(10)	N1−Cu1−Cl1	100.98(8)
Cu1−O1−Cu1*1	99.15(12)	Cu1−O2−Cu1*1	103.37(2)

[a] *1, $-x, {}^1/_2 - y, z$; *2, ${}^1/_4 - y, {}^1/_4 + x, {}^1/_4 - z$; *3, $-{}^1/_4 + y, {}^1/_4 - x, {}^1/_4 - z$.

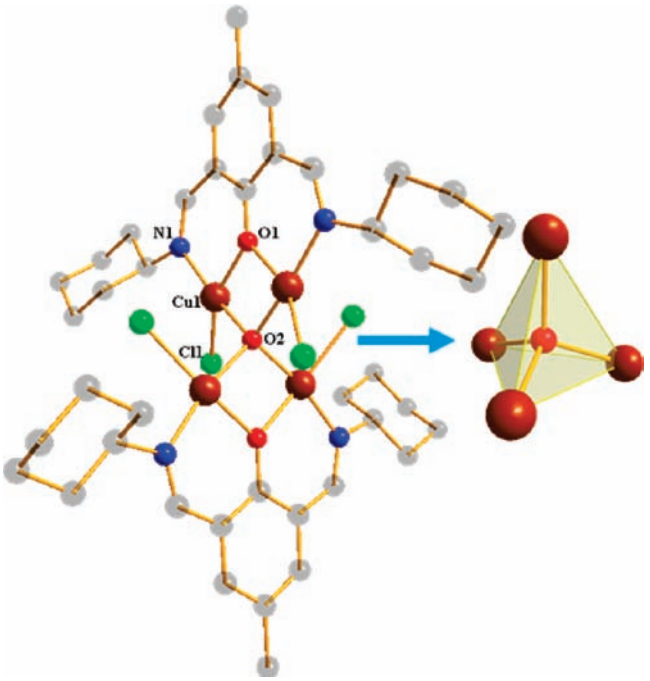

Figure 2. Molecular structure of $[Cu_4(\mu_4\text{-}O)(\mu\text{-}cip)_2Cl_4]$ in **1** with an atom numbering scheme with a $[Cu_4]$ tetrahedron arrangement.

Description of Structures. *$[Cu_4(\mu_4\text{-}O)(\mu\text{-}cip)_2Cl_4]$ (**1**).* Compound **1** crystallizes in the tetragonal centrosymmetric $I4_1/a$ space group with four molecules in the unit cell without any interstitial solvent molecule. The molecular structure of **1** is shown in Figure 1, and selected bond lengths and angles are given in Table 2. **1** is composed of neutral molecules consisting of two deprotonated cip^- ligands, each providing a N_2O set of donor atoms to the $[Cu_4]$ core that is assembled around a central μ_4-O group. Four chloride anions complete the square-planar coordination spheres around the Cu^{II} metal ions (Figure 2). Four equivalent copper atoms are located at the corners of an almost regular tetrahedron centered on a O^{2-} anion, O2, and with Cu···Cu edges varying from 2.99 to 3.18 Å. The previously reported tetranuclear copper(II) complexes possessing the $[Cu_4(\mu_4\text{-}O)]^{6+}$ tetrahedral core are known to have phenoxido and other supports for the oxido core.[28]

dx.doi.org/10.1021/ic102226j |*Inorg. Chem.* 2011, 50, 3922–3933

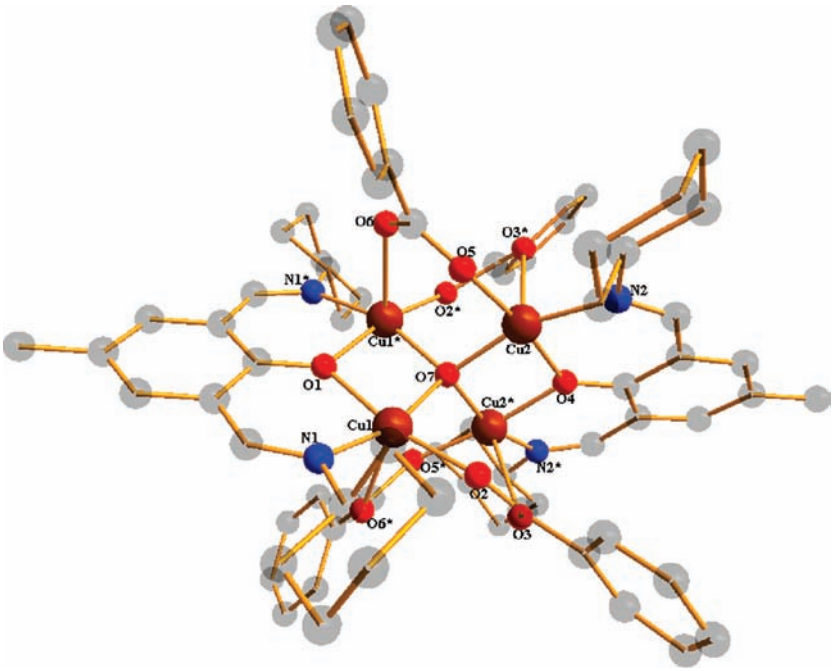

Figure 3. Molecular structure of $[Cu_4(\mu_4\text{-}O)(\mu\text{-cip})_2)(\mu_{1,3}\text{-}O_2CPh)_4]$ in $\mathbf{2}\cdot 2CH_3OH$ with an atom numbering scheme. H atoms are omitted for clarity.

The square-planar coordination sphere of the Cu1 site is occupied by one imine N1 atom and one O1 atom of a deprotonated cip$^-$ ligand, one Cl1 atom, and the μ_4-O2 center (Figure S2 in the Supporting Information). Only two of the six edges of the $[Cu_4]$ tetrahedron are supported by phenoxido bridges (O11), while the other edges remain unsupported (Figure S3 in the Supporting Information). Apart from the phenoxido O1 and the central O2 bridges, no other additional supports are needed to ensure stability to the tetrahedron core. The phenoxido-bridged $[Cu_2]$ fragments present a Cu···Cu distance of 2.995 Å, which is much shorter than the unbridged edges with long Cu···Cu distances of around ~3.18 Å (av.). It is worth mentioning for comparison that we reported earlier a tetranuclear copper(II) complex, $[Cu_4(\mu_4\text{-}O)(bahped)_2](ClO_4)_2$, containing only a μ_4-oxido bridge (i.e., without any carboxylate or phenoxido bridge along the six tetrahedral edges) to assemble the tetrahedron core.[23] In **1**, the Cu^{II} site adopts in square-planar (*spl*) geometry without any kind of *apical* interactions to the Cl$^-$ groups. Around the distorted square plane of the Cu^{II} site, *trans* positions are occupied by N1 and the central O2 with a N1−Cu1−O2 angle of 169.99° and the phenoxide O1 and Cl1 atoms with a O1−Cu1−Cl1 angle of 158.20° (Figure S2 in the Supporting Information). The Cu1−Cl1 bond length in the *basal* plane (2.244 Å) is longer than that of Cu1−μ_4-O2 (1.908 Å) and the Cu1−$O1_{ph}$ (1.967 Å) and Cu−$N1_{im}$ (1.968 Å) bond lengths. The Cu1−$O1_{ph}$−Cu1 angle spans about 99.1°. The phenoxido oxygen bridge squeezes the Cu−μ_4-O−Cu (Cu1−O2−Cu1*1 and Cu1*2−O2−Cu1*3) angles to 103.4° compared to the other angles at 112.6° (Cu1−O2−Cu1*3 and Cu1*1−O2−Cu1*2). All of these distances and angles are in good agreement with the literature values.[29] Two phenoxido-bridged $[Cu_2]$ fragments stay exactly perpendicular to each other with a dihedral angle of 90° between the two Cu_2O_2 planes. All of the *cyclo*-hexyl rings adopt a *chair* conformation with the equatorial N1 atom of the cip- ligands after condensing as imine bonds. In crystal packing, no hydrogen-bonding network has been identified. The crystal-packing diagram along the *b* axis is shown in Figure S4 in the Supporting Information.

Table 3. Selected Interatomic Distances (Å) and Angles (deg) for Complex $\mathbf{2}\cdot 2CH_3OH$[a]

Distances			
O7−Cu2*	1.9150(19)	O2−Cu1	1.952(2)
O7−Cu2	1.9150(19)	O3−Cu2*	2.343(3)
O7−Cu1	1.9179(19)	Cu1−N1	2.000(3)
O7−Cu1*	1.9179(19)	Cu1−O6*	2.325(3)
O1−Cu1	1.975(2)	Cu1−Cu1*	3.0105(8)
O1−Cu1*	1.975(2)	Cu2−O5	1.952(2)
O4−Cu2	1.965(2)	Cu2−N2	1.991(3)
O4−Cu2*	1.965(2)	Cu2−O3*	2.343(3)
O6−Cu1*	2.325(3)	Cu2−Cu2*	2.9929(8)
Angles			
O7−Cu1−O2	92.77(10)	O7−Cu2−O5	93.68(11)
O7−Cu1−O1	78.63(10)	O7−Cu2−O4	79.01(10)
O2−Cu1−O1	168.93(10)	O5−Cu2−O4	172.27(11)
O7−Cu1−N1	162.08(9)	O7−Cu2−N2	162.06(9)
O2−Cu1−N1	95.31(11)	O5−Cu2−N2	95.31(11)
O1−Cu1−N1	91.12(10)	O4−Cu2−N2	91.06(11)
O7−Cu1−O6*	98.83(6)	O7−Cu2−O3*	96.48(7)
O2−Cu1−O6*	98.72(11)	O5−Cu2−O3*	98.27(11)
O1−Cu1−O6*	89.57(7)	O4−Cu2−O3*	85.19(8)
N1−Cu1−O6*	95.72(10)	N2−Cu2−O3*	97.54(10)
Cu1−O1−Cu1*	99.31(14)	Cu1−O7−Cu1*	103.19(14)
Cu2−O4−Cu2*	99.21(14)	Cu2−O7−Cu2*	102.80(14)

[a] * = 1 − *x*, *y*, $^1/_2$ − *z*.

$[Cu_4(\mu\text{-cip})_2(\mu_4\text{-}O)(\mu_{1,3}\text{-}O_2CPh)_4]\cdot 2CH_3OH$ ($\mathbf{2}\cdot 2CH_3OH$). The molecular structure of complex **2** is given in Figure 3, and

dx.doi.org/10.1021/ic102226j |*Inorg. Chem.* 2011, 50, 3922–3933

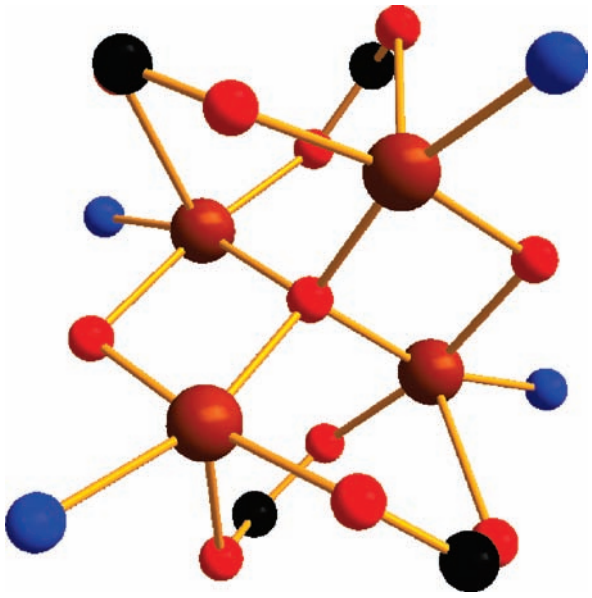

Figure 4. Partial molecular structure of **2**·2CH_3OH highlighting the polynuclear coordination core.

important bond lengths and angles for **2** are listed in Table 3. **2**·2CH_3OH crystallizes in the monoclinic *C*2/*c* space group with a crystallographic inversion center located on the O7 atom, implying that the asymmetric unit contains half of a tetranuclear molecule and one CH_3OH molecule. **2** is composed of neutral complexes consisting of two deprotonated cip^- ligands, each providing N_2O donor atoms to the $[Cu_4]$ core that is assembled by a central μ_4-O7 group. Four benzoate groups complete the coordination sphere of the Cu^{II} centers (Figures 3 and 4). The four Cu^{II} centers arrange around the central μ_4-O^{2-} anion in a distorted T_d geometry, with Cu···Cu distances varying from 2.99 to 3.19 Å, which are significantly longer than those in the known benzoate-bridged copper paddlewheel dimers (Figure S5 in the Supporting Information).[30] The Cu^{II} coordination spheres display a distorted square-based pyramid (*spy*) geometry consisting of two O atoms of bridging carboxylate anions, one phenoxido O atom, one central O^{2-} anion, and one N atom of the cip^- imine group (Figure S6 in the Supporting Information). The square base is occupied in a trans fashion by the N atom and the central O^{2-} anion with N−Cu−O angles of 162.06−162.08° and by a phenoxido atom and one carboxylato O atom with O−Cu−O angles of 168.93−172.24°. The *spy* geometry is completed by the second carboxylato O atom bound to the *apical* Cu^{II} positions, with bond distances of 2.32−2.34 Å that are longer by 0.3−0.4 Å than those found in the basal plane: Cu−O_{bz} (bz = benzoate) ≈ 1.95 Å; Cu−μ_4-O ≈ 1.91 Å; Cu−O_{ph} ≈ 1.96−1.97 Å; Cu−N_{im} ≈ 1.99−2.00 Å. The Cu atoms are shifted by about 0.15−0.20 Å from their least-squares *basal* planes toward the *apical* carboxylato O atoms. The four benzoato groups are bridging Cu^{II} metal ions along two edges of the $[Cu_4O]$ tetrahedron, while the phenoxido groups connect two other edges (Figures 3 and S7 in the Supporting Information). Thus, only two edges remain unsupported, leaving the $[Cu_4O]$ tetrahedron less open than in **1**. All of the benzoato groups coordinate uniformly in the *apical*−*equatorial* positions of the Cu^{II} sites (Figures 3 and S8 in the Supporting Information). The Cu−O−C−O/O−C−O−Cu torsion angles (6.63/36.57°) indicate that the benzoate groups bridge the Cu^{II} metal ions in a syn−syn mode (ideal values 0°/0°) with a slightly *out-of-plane* binding for the second Cu atom. Within the $[Cu_2(\mu\text{-cip})]^{3+}$ units, the phenoxido O atom is bridging Cu^{II} ions in only equatorial positions. The Cu−O_{ph}−Cu angles span about 99.2°, squeezing the Cu−μ_4-O−Cu (Cu1−O7−Cu1* and Cu2−O7−Cu2*) angles to 103.09° in comparison to the Cu1−O7−Cu2* and Cu2−O7−Cu1* angles of 112.86°, which are in good agreement with the literature values.[31,32] The dihedral angle between the two Cu_2O_2 planes of the phenoxido-bridged $[Cu_2]$ fragments is 89.83°, indicating a distortion similar to that observed for **1**. The Addison τ parameter for the Cu^{II} centers falls within the 0.11−0.17 range, highlighting only a slight *tbp* (trigonal-bipyramid) distortion from ideal *spy* geometry.[33] The Cu^{II} ions in phenoxido-bridged $[Cu_2]$ fragments are separated by about 3.00 Å, which is shorter than the 3.189 Å Cu···Cu distance in benzoato-bridged moieties. The longest Cu···Cu distances, ∼3.194 Å, are found for the Cu^{II} ions unbridged along the tetrahedral edge. O atoms of the interstitial CH_3OH molecules are involved in intermolecular hydrogen-bonding interactions with two benzoato O atoms (Figure S9 in the Supporting Information). The crystal packing along the *a* axis is shown in Figure S10 (see the Supporting Information).

*$[Cu_4(\mu_{1,1}\text{-}N_3)_4(\mu\text{-cip})_2(N_3)_2]$·DMF (**3**·DMF).* The molecular structure of $[Cu_2(\mu_{1,1}\text{-}N_3)_2(\mu\text{-cip})(N_3)]_2$ is shown in Figure 5, and selected bond lengths and angles are listed in Table 4. **3** crystallizes in the *C*2/*c* space group, and the asymmetric unit contains only half of the tetranuclear complex, with the second half being generated by the $(-x, y, 0.5 - z)^*$ symmetry operator. The neutral centrosymmetrical $[Cu_4]$ complex **3** is composed of two $[Cu_2(\mu_{1,1}\text{-}N_3)_2(\mu\text{-cip})(N_3)]$ fragments that are assembled by two $\mu_{1,1}$-azido bridges (N9 and N9*) between Cu2 and Cu1* and between Cu2* and Cu1 in an equatorial−axial binding mode (Figure 5). In the formed $[Cu_4]$ rhomboidal complex, the two $\mu_{1,1}$-N_3^- (N3 and N3*) anions that bridge Cu1 and Cu2 in their basal planes have obviously replaced the central μ_4-O group present in **1** and **2**. The resulting azido- and phenoxido-bridged $[Cu_4]$ rhomboidal core structure is not known in the literature. This structure is different from the double cubane structure because the azido bridges (N3 and N3*) within the core of the rhomboidal structure are only of the bridging type. In the $[Cu_2(\mu_{1,1}\text{-}N_3)_2(\mu\text{-cip})(N_3)]$ moieties, the deprotonated cip^- ligand provides a N_2O set of donor atoms to the two Cu^{II} sites (Cu···Cu distance of 3.121 Å) that are sharing the bridging phenoxido O1 atom. While Cu2 adopts a square-planar (*sp*) geometry, Cu1 exhibits a distorted square-based pyramid (*spy*) coordination sphere. The square plane of Cu2 is occupied by two N atoms (N9 and N3) of the bridging azide anions, N2 and O1 atoms from respectively the imine and phenoxido groups of the cip^- ligand (Figure S11 in the Supporting Information). It is worth mentioning that Cu2 is displaced by 0.075 Å from the mean N9−N3−O1−N2 plane and that the free *apical* position of square-planar Cu2 atom shows interaction with formyl O atoms of disordered DMF molecules at 2.518 Å. The square base of Cu1 is occupied by N1 and O1 atoms from respectively the imine and phenoxido groups of the cip^- ligand and two N atoms (N6 from a terminal azide ligand and N3) of azide anions. Cu1 displaced by 0.236 Å from the N6−N3−O1−N1 mean basal plane. The distortion of the *spy* geometry around Cu1 is larger than that observed in **2** with an Addison parameter of 0.35. In the basal plane of both Cu sites, the imine N1 or N2 atom is coordinating to Cu^{II} in the trans position of the bridging azido N3 atom with N−Cu−N3 angles of 167.35 and 168.45°.

dx.doi.org/10.1021/ic102226j |*Inorg. Chem.* 2011, 50, 3922–3933

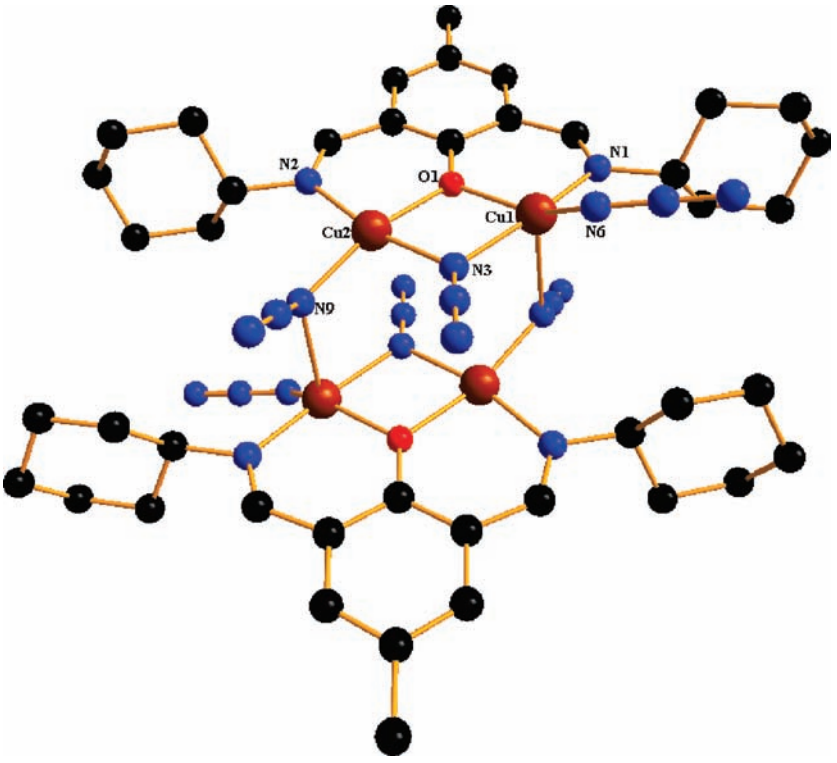

Figure 5. Molecular structure of $[Cu_4(\mu\text{-}N_3)_4(\mu\text{-cip})_2(N_3)_2]$ in **3**·DMF with an atom numbering scheme. H atoms are omitted for clarity.

Table 4. Selected Interatomic Distances (Å) and Angles (deg) for Complex 3·DMF[a]

	Distances		
Cu1−N6	1.943(3)	Cu2−N2	1.968(2)
Cu1−N1	1.953(2)	Cu2−N3	1.978(3)
Cu1−N3	1.994(2)	Cu2−O1	1.9809(19)
Cu1−O1	2.0147(19)	Cu2−N9	1.966(3)
Cu1−N9*	2.429(3)		
	Angles		
N6−Cu1−N1	101.85(12)	N3−Cu1−N9*	85.27(11)
N6−Cu1−N3	90.80(12)	O1−Cu1−N9*	90.03(9)
N1−Cu1−N3	167.35(11)	N9−Cu2−N2	96.10(11)
N6−Cu1−O1	145.88(14)	N9−Cu2−N3	95.13(11)
N1−Cu1−O1	92.89(9)	N2−Cu2−N3	168.45(11)
N3−Cu1−O1	76.19(9)	N9−Cu2−O1	165.02(10)
N6−Cu1−N9*	120.65(15)	N2−Cu2−O1	92.31(9)
N1−Cu1−N9*	88.41(10)	N3−Cu2−O1	77.34(9)
Cu1−O1−Cu2	102.73(9)	Cu1−N3−Cu2	103.61(11)
Cu1−N9*−Cu2*	105.61(11)		

[a] * = $-x$, $1-y$, $1-z$.

Similarly, the phenoxido O1 and monodentate azide N6 or bridging azide N9 atoms are trans to each other with O1−Cu−N angles of 145.88 and 165.02°. The Cu−N_{az} (az = azide) bond lengths involving a Cu^{II} *basal* plane (av. 1.98 Å) are shorter than the Cu1−$N9_{az}$* bond distance (2.429 Å) in the *axial* direction due to the Jahn−Teller effect and longer than the Cu1−$N6_{az}$ one at 1.943 Å in the case of the monodentate azide anion (Figure S11 in the Supporting Information). Within the rhomboidal $[Cu_4]$ arrangement, the four Cu atoms are coplanar with Cu1···Cu2 = 3.121 Å and Cu1···Cu2* = 3.512 Å (Figure S12 in the Supporting Information) and with short Cu2···Cu2* = 3.659 Å and long Cu1···Cu1* = 5.546 Å diagonals (Figure S13 in the Supporting Information).

Magnetic Properties. The solid-state magnetic properties of **1**, **2**·2CH_3OH, and **3**·DMF have been investigated using dc susceptibility measurements in the 1.8−300 K temperature range under a magnetic field of 1000 Oe (Figure 5). At 300 K, the χT products are 0.22, 0.49, and 0.68 cm^3 K mol^{-1} for **1**−**3**, respectively. These χT values are far from the theoretical value of 1.5 cm^3 K mol^{-1} expected for four isolated paramagnetic Cu^{2+} ions (d^9, $S = {}^1/_2$) with $g = 2$, indicating that strong and dominant antiferromagnetic interactions exist between the Cu^{2+} ions in these complexes. Upon cooling, the χT products continuously decrease to reach a value close to zero below 120, 80, and 70 K for **1**−**3**, respectively.

Generally speaking, for the Cu^{II} ions, the magnetic interactions mediated through their *axial* positions are much weaker than those mediated by their *equatorial* sites. Therefore, if one considers only the magnetic pathways that involve equatorial bonds around each Cu^{II} ion, **3** can be viewed as two almost isolated Cu1−Cu2 dinuclear units with a double phenoxido−azido bridge (Figure 5). For **1** and **2**, the situation is slightly different because of the presence of the central μ_4-oxido bridge between Cu^{II} ions. Nevertheless, the magnetic pathway through the double μ_4-oxido−phenoxido bridges is likely much more efficient than a single μ_4-oxido bridge between two Cu^{II} metal ions. As a consequence, the magnetic description of **1** and **2** with two isolated dinuclear units with a double phenoxido−oxido bridge (Figures 2 and 3) is similar to that of **3** (vide supra). For **1** like for **3**, only one spin dimer has to be considered. For **2**, considering the similarity of the bridging modes in the two

dx.doi.org/10.1021/ic102226j |*Inorg. Chem.* 2011, 50, 3922–3933

dinuclear [Cu_2] units (Table 3), the interaction in the two spin dimers is expected to be similar. Considering these magnetostructural remarks, the magnetic properties of the three compounds can be analyzed in a first approximation with the same magnetic model including two identical $S = {}^1/_2$ spin dimers with only one exchange parameter, denoted as J. The magnetic susceptibility has thus been calculated from the following isotropic spin Heisenberg−Hamiltonian:

$$H = -2J\{S_{Cu,1} \cdot S_{Cu,2}\} \quad (7)$$

where S_i are the spin operators for each center with $S = {}^1/_2$. Application of the van Vleck equation[34,35] allows the determination of the low-field analytical expression of the magnetic susceptibility[36] taking into account the presence of a residual extrinsic paramagnetic contribution:

$$\chi T = 2(1-\rho)\frac{2N\mu_B{}^2 g_{Cu}{}^2}{k_B}\frac{1}{3+e^{-2J/k_BT}} + \rho\frac{N\mu_B{}^2 g_{Cu}{}^2}{4k_B} \quad (8)$$

As shown in Figure 6, the above expression of the magnetic susceptibility reproduces almost perfectly the experimental χT vs T data at 1000 Oe. The best sets of parameters obtained are given in Table 5 for the three compounds. The negative sign of the magnetic interaction implies that these Cu^{II} dimer units and thus

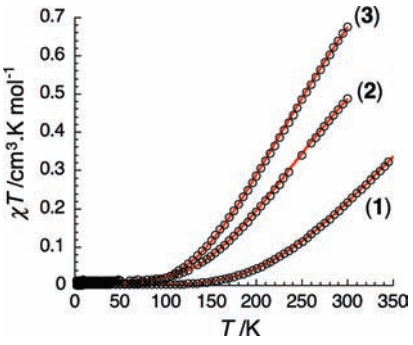

Figure 6. Temperature dependence of the χT product (with χ being the molar magnetic susceptibility defined as M/H) for **1**, **2**·2CH_3OH, and **3**·DMF. The solid lines are the best fit obtained using the isotropic dinuclear $S = {}^1/_2$ Heisenberg model described in the text.

Table 5. Parameters Deduced from Analysis of the Magnetic Properties for 1, 2·2CH_3OH, and 3·DMF

	g	J/k_B (K)	ρ (%)
1	2.2(1)	−513(15)	0
2	2.03(10)	−340(10)	3
3	2.3(1)	−315(5)	2

the tetranuclear complexes possess an $S_T = 0$ spin ground state, i.e., a diamagnetic ground state. The ρ values indicate that a very small amount of residual paramagnetic contribution is present in the measured samples of **1** and **3**, as it is seen for materials displaying a diamagnetic ground state. Taking into account that the impurity possesses a Curie S = 1/2 paramagnetic behavior and the same molecular weight as the major complex, the amount is about 3 and 2% for **2** and **3**, respectively.

It is worth mentioning that the magnetic properties of these complexes have also been analyzed with an alternative model including two different intramolecular interactions. For **1** and **2**, one could consider one interaction mediated by the double oxido−phenoxido bridges and the another one mediated by a single μ_4-oxido bridge.[37] Indeed, as soon as two interactions are considered in the model, more than one set of parameters can reproduce well the experimental data, suggesting an overparametrization of the fitting procedures. Therefore, the only relevant model requires no more than one interaction parameter, as shown in Figure 7, and thus it is not possible to evaluate the magnetic interaction through the single μ_4-oxido bridge in **1** and **2** or the single azido bridges in **3**. The amplitude of the antiferromagnetic exchange parameter is relatively large for the three compounds but stays in the range of magnitude observed in similar compounds with the same type of double oxido−phenoxido or azido−phenoxido bridges.[38−40] It is well known that alkoxido−phenoxido-bridged Cu_2 complexes show antiferromagnetic interaction when the Cu−$O_{phenoxido/alkoxido}$−Cu angle is larger than 97.6°, and the antiferromagnetic interaction increases with increasing angle.[41] Thus, in the present case, in all three complexes having Cu−$O_{phenoxido}$−Cu and Cu−$O_{alkoxido}$−Cu angles close to 99° and 103°, respectively, the coupling through the alkoxido−phenoxido group should be antiferromagnetic. On the other hand, the ferromagnetic interaction for $\mu_{1,1}$-N_3 bridges decreases with an increase in the Cu−N_{azido}−Cu angle from 85° and can exhibit antiferromagnetic behavior for a Cu−N_{azido}−Cu angle ≥104°.[42] In complex **3**, the Cu−N_{azido}−Cu and Cu−$O_{phenoxido}$−Cu angles (102.73° and 103.61°) are close to the cutoff value of 104° for ferromagnetic character, and very weak ferromagnetic coupling may be expected through the bridging azido group. Experimentally, this weak ferromagnetic interaction is indeed dominated by the strong antiferromagnetic coupling mediated by the phenoxido bridge.

Concluding Remarks. The coordination chemistry of the cip^- ligand has been studied and confirms the key role played by the ancillary ligands in the synthesis of three new tetranuclear copper(II) complexes. Chloride, benzoate, and azide ligands have been used to control the molecular topology of the final [Cu_4] products. The tridentate cip^- ligand facilitates the trapping of two Cu^{II} pairs, leaving available coordinating sites for the binding of oxido, benzoato, and azido anions, which help

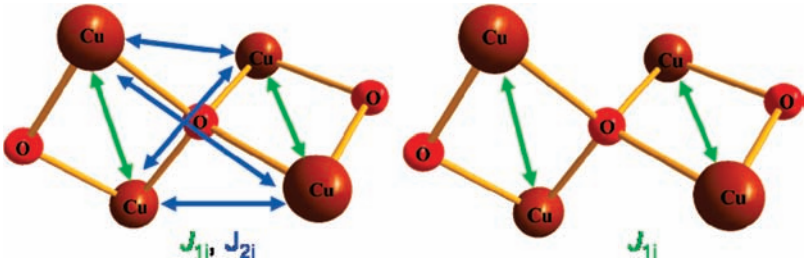

Figure 7. Magnetic cores of **1** and **2**.

dx.doi.org/10.1021/ic102226j |Inorg. Chem. 2011, 50, 3922–3933

the assembly of two Cu^{II} pairs in tetrahedral and rhomboidal molecular topologies. Spontaneous conversions and ancillary ligand-exchange reactions allowed us to study the binding efficiency of N_3^- and $PhCO_2^-$ over Cl^-, suggesting a rational synthetic approach to the synthesis of tetranuclear complexes. We are currently working on other ancillary bridges such as O^{2-}, O_2^{2-}, S^{2-}, HS^-, etc., in this reaction system to induce the formation of new types of homo- and heterometallic assembled cage complexes.

■ ASSOCIATED CONTENT

Supporting Information. X-ray crystallographic data in CIF format, Scheme S1, Figures S1−S13, and synthesis and characterization of ligand Hcip. This material is available free of charge via the Internet at http://pubs.acs.org.

■ AUTHOR INFORMATION

Corresponding Author

* E-mail: clerac@crpp-bordeaux.cnrs.fr (R.C.), dray@chem.iitkgp.ernet.in (D.R.). Tel: (+33) 5 56 84 56 50 (R.C.), (+91) 3222-283324 (D.R.). Fax: (+33) 5 56 84 56 00 (R.C.), (+91) 3222-82252 (D.R.).

■ ACKNOWLEDGMENT

M.S. is thankful to the Council of Scientific and Industrial Research, New Delhi, India, for financial support. V.B. acknowledges the Italian Ministry of University and Scientific Research (MIUR, Rome). R.C., C.M., and N.G.R.H. thank the University of Bordeaux, the CNRS, and the Region Aquitaine, GIS Advanced Materials in Aquitaine (COMET Project), for funding and the Natural Science and Engineering Council of Canada for a year of a postdoctoral fellowship.

■ REFERENCES

(1) Coronado, E.; Dunbar, K. R. *Inorg. Chem.* **2009**, *48*, 3293–3295.
(2) Maiti, D.; Woertink, J. S.; Ghiladi, R. A.; Solomon, E. I.; Karlin, K. D. *Inorg. Chem.* **2009**, *48*, 8342–8356.
(3) Alemayehu, A. B.; Gonzalez, E.; Hansen, L. K.; Ghosh, A. *Inorg. Chem.* **2009**, *48*, 7794–7799.
(4) Paital, A. R.; Wu, A.-Q.; Guo, G.-C.; Aromí, G.; Ribas-Ariño, J.; Ray, D. *Inorg. Chem.* **2007**, *46*, 2947–2949.
(5) Banerjee, A.; Sarkar, S.; Chopra, D.; Colacio, E.; Rajak, K. K. *Inorg. Chem.* **2008**, *47*, 4023–4031.
(6) Paital, A. R.; Mitra, T.; Ray, D.; Wong, W. T.; Ribas-Ariño, J.; Novoa, J. J.; Ribas, J.; Aromí, G. *Chem. Commun.* **2005**, 5172–5174.
(7) Paital, A. R.; Mandal, D.; Huang, X.; Li, J.; Aromí, G.; Ray, D. *Dalton Trans.* **2009**, 1352–1362.
(8) Paital, A. R.; Bertolasi, V.; Aromí, G.; Ribas-Ariño, J.; Ray, D. *Dalton Trans.* **2008**, 861–864.
(9) Paital, A. R.; Hong, C. S.; Kim, H. C.; Ray, D. *Eur. J. Inorg. Chem.* **2007**, 1644–1653.
(10) Nanda, P. K.; Aromí, G.; Ray, D. *Chem. Commun.* **2006**, 3181–3183.
(11) Paital, A. R.; Nanda, P. K.; Das, S.; Aromí, G.; Ray, D. *Inorg. Chem.* **2006**, *45*, 505–507.
(12) Nanda, P. K.; Aromí, G.; Ray, D. *Inorg. Chem.* **2006**, *45*, 3143–3145.
(13) Cheng, X.-N.; Xue, W.; Huang, J.-H.; Chen, X.-M. *Dalton Trans.* **2009**, 5701–5707.
(14) Ghosh, A. K.; Ghoshal, D.; Zangrando, E.; Ribas, J.; Chaudhuri, N. R. *Inorg. Chem.* **2007**, *46*, 3057–3071.
(15) Biswas, C.; Mukherjee, P.; Drew, M. G. B.; Gomez-Garcia, C. J.; Clemente-Juan, J. M.; Ghosh, A. *Inorg. Chem.* **2007**, *46*, 10771–10780.
(16) (a) Ribas, J.; Escuer, A.; Monfort, M.; Vicente, R.; Cortes, R.; Lezama, L.; Rojo, T. *Coord. Chem. Rev.* **1999**, *193*−*195*, 1027–1068. (b) Mukherjee, P. S.; Dalai, S.; Mostafa, G.; Lu, T.-H.; Rentschler, E.; Chaudhuri, N. R. *New J. Chem.* **2001**, *25*, 1203–1207. (c) Ray, M. S.; Ghosh, A.; Chaudhuri, S.; Drew, M. G. B.; Ribas, J. *Eur. J. Inorg. Chem.* **2004**, 3110–3117. (d) Zbiri, M.; Saha, S.; Adhikary, C.; Chaudhuri, S.; Daul, C.; Koner, S. *Inorg. Chim. Acta* **2006**, *359*, 1193–1199. (e) Koner, S.; Saha, S.; Mallah, T.; Okamoto, K.-I. *Inorg. Chem.* **2004**, *43*, 840–842. (f) Ray, M. S.; Ghosh, A.; Bhattacharya, R.; Mukhopadhyay, G.; Drew, M. G. B.; Ribas, J. *Dalton Trans.* **2004**, 252–259. (g) Naiya, S.; Biswas, C.; Drew, M. G. B.; Gómez-García, C. J.; Clemente-Juan, J. M.; Ghosh, A. *Inorg. Chem.* **2010**, *49*, 6616–6627.
(17) Kwit, M.; Gawronski, J. *Tetrahedron: Asymmetry* **2003**, *14*, 1303–1308.
(18) Mandal, D.; Ray, D. *Inorg. Chem. Commun.* **2007**, *10*, 1202–1205.
(19) Mandal, D.; Bertolasi, V.; Ribas-Ariño, J.; Aromí, G.; Ray, D. *Inorg. Chem.* **2008**, *47*, 3465–3467.
(20) Shiga, T.; Maruyama, K.; Han, L. Q.; Oshio, H. *Chem. Lett.* **2005**, *34*, 1648–1649.
(21) Yamashita, S.; Shiga, T.; Kurashina, M.; Nihei, M.; Nojiri, H.; Sawa, H.; Kakiuchi, T.; Oshio, H. *Inorg. Chem.* **2007**, *46*, 3810–3812.
(22) Nakamoto, K. *Infrared and Raman Spectra of Inorganic and Coordination Compounds, part B*; John Wiley & Sons: New York, 1997; pp 59−62 and 276−282.
(23) Bera, M.; Wong, W. T.; Aromí, G.; Ribas, J.; Ray, D. *Inorg. Chem.* **2004**, *43*, 4787–4789.
(24) Guy, J. T., Jr.; Cooper, J. C.; Gilardi, R. D.; Flippen-Anderson, J. L.; George, C. F., Jr. *Inorg. Chem.* **1988**, *27*, 635–638.
(25) Teipel, S.; Griesar, K.; Haase, W.; Krebs, B. *Inorg. Chem.* **1994**, *33*, 456–464.
(26) Lazari, G.; Stamatatos, T. C.; Raptopoulou, C. P.; Psycharis, V.; Pissas, M.; Perlepes, S. P.; Boudalis, A. K. *Dalton Trans.* **2009**, 3215–3221.
(27) Lahiri, D.; Bhowmick, T.; Pathak, B.; Shameema, O.; Patra, A. K.; Ramakumar, S.; Chakravarty, A. R. *Inorg. Chem.* **2009**, *48*, 339–349.
(28) (a) Arnold, P. L.; Rodden, M.; Davis, K. M.; Scarisbrick, A. C.; Blake, A. J.; Wilson, C. *Chem. Commun.* **2004**, 1612–1613. (b) Richardson, C.; Steel, P. J. *Dalton Trans.* **2003**, 992–1000. (c) McKee, V.; Tandon, S. S. *J. Chem. Soc., Dalton Trans.* **1991**, 221–230. (d) Blake, A. J.; Grant, C. M.; Gregory, C. I.; Parsons, S.; Rawson, J. M.; Reed, D.; Winpenny, R. E. P. *J. Chem. Soc., Dalton Trans.* **1995**, 163–175. (e) Duncan, P. C. M.; Goodgame, D. M. L.; Hitchman, M. A.; Menzer, S.; Stratemeier, H.; Williams, D. J. *J. Chem. Soc., Dalton Trans.* **1996**, 4245–4248. (f) Mukherjee, S.; Weyhermüller, T.; Bothe, E.; Wieghardt, K.; Chaudhuri, P. *Eur. J. Inorg. Chem.* **2003**, 863–875. (g) Martin, J. L., Jr.; Yuan, J.; Lunte, C. E.; Elder, R. C.; Heineman, W. R.; Deutsch, E. *Inorg. Chem.* **1989**, *28*, 2901–2902. (h) Chen, L.; Breeze, S. R.; Rousseau, R. J.; Wang, S.; Thompson, L. K. *Inorg. Chem.* **1995**, *34*, 454–465. (i) El-Toukhy, A.; Cai, G.-Z.; Davies, G.; Gilbert, T. R.; Onan, K. D.; Veidis, M. *J. Am. Chem. Soc.* **1984**, *106*, 4596–4605.
(29) Reim, J.; Griesar, K.; Haase, W.; Krebs, B. *J. Chem. Soc., Dalton Trans.* **1995**, 2649–2656.
(30) Takamizawa, S.; Miyake, R. *Chem. Commun.* **2009**, 4076–4078.
(31) Roy, P.; Nandi, M.; Manassero, M.; Riccó, M.; Mazzani, M.; Bhaumik, A.; Banerjee, P. *Dalton Trans.* **2009**, 9543–9554.
(32) Shakya, R.; Keyes, P. H.; Heeg, M. J.; Moussawel, A.; Heiney, P. A.; Verani, C. N. *Inorg. Chem.* **2006**, *45*, 7587–7589.
(33) Addison, A. W.; Rao, T. N.; Reedijk, J.; Rijn, J.; van Verschoor, G. V. *J. Chem. Soc., Dalton Trans.* **1984**, 1349–1356.
(34) van Vleck, J. H. *The Theory of Electric and Magnetic Susceptibility*; Oxford University Press: Oxford, U.K., 1932.
(35) Kambe, K. *J. Phys. Soc. Jpn.* **1950**, *5*, 48–51.
(36) O'Connor, C. J. *Prog. Inorg. Chem.* **1982**, *29*, 203–283.

(37) Hall, J. W.; Estes, W. E.; Estes, E. D.; Scaringe, R. P.; Hatfield, W. E. *Inorg. Chem.* **1977**, *16*, 1572–1574.
(38) Adams, A.; Fenton, D. E.; Haque, S. R.; Heath, S.; Ohba, M.; Okawa, H.; Spey, S. E. *Dalton Trans.* **2000**, 1849–1856.
(39) Banerjee, A.; Sarkar, S.; Chopra, D.; Colacio, E.; Rajak, K. K. *Inorg. Chem.* **2008**, *47*, 4023–4031.
(40) Sarkar, M.; Clérac, R.; Mathonière, C.; Hearns, N. H.; Bertolasi, V.; Ray, D. *Inorg. Chem.* **2010**, *49*, 6575–6585.
(41) Crawford, V. H.; Richardson, H. W.; Hodgson, J. R.; Wasson, D. J.; Hatfield, W. E. *Inorg. Chem.* **1976**, *15*, 2107–2110.
(42) Ruiz, E.; Cano, J.; Alvarez, S.; Alemany, P. *J. Am. Chem. Soc.* **1998**, *120*, 11122–11129.